BIOCHEMISTRY

BRD4 methylation by the methyltransferase SETD6 regulates selective transcription to control mRNA translation

Zlata Vershinin[1,2], Michal Feldman[1,2], Thilo Werner[3], Lital Estrella Weil[1,2], Margarita Kublanovsky[1,2], Elina Abaev-Schneiderman[1,2], Menachem Sklarz[2], Enid Y. N. Lam[4], Khawla Alasad[2,5], Sarah Picaud[6], Barak Rotblat[2,5], Ruth A. McAdam[7], Vered Chalifa-Caspi[2], Marcus Bantscheff[3], Trevor Chapman[7], Huw D. Lewis[7], Panagis Filippakopoulos[6], Mark A. Dawson[4], Paola Grandi[3], Rab K. Prinjha[7], Dan Levy[1,2]*

The transcriptional coactivator BRD4 has a fundamental role in transcription regulation and thus became a promising epigenetic therapeutic candidate to target diverse pathologies. However, the regulation of BRD4 by posttranslational modifications has been largely unexplored. Here, we show that BRD4 is methylated on chromatin at lysine-99 by the protein lysine methyltransferase SETD6. BRD4 methylation negatively regulates the expression of genes that are involved in translation and inhibits total mRNA translation in cells. Mechanistically, we provide evidence that supports a model where BRD4 methylation by SETD6 does not have a direct role in the association with acetylated histone H4 at chromatin. However, this methylation specifically determines the recruitment of the transcription factor E2F1 to selected target genes that are involved in mRNA translation. Together, our findings reveal a previously unknown molecular mechanism for BRD4 methylation–dependent gene-specific targeting, which may serve as a new direction for the development of therapeutic applications.

INTRODUCTION

The transcription regulator BRD4 is a member of the bromodomain and extraterminal domain (BET) protein family. BRD4 contains two conserved bromodomains (*1*, *2*) that specifically recognize acetylated lysine residues on histone and non-histone proteins (*3*–*7*). This binding is known to regulate transcription of target genes involved in a wide range of biological processes and diseases (*3*–*5*, *8*). The critical role of BRD4 in the transcription process marks it as an attractive candidate for pharmacological intervention. BET inhibitors, targeting BRD family members and displacing them from chromatin, were studied extensively in different malignancies in recent years, demonstrating a notable therapeutic potential (*4*, *8*–*16*). However, little is known about their regulation by posttranslational modifications.

Lysine methylation, catalyzed by protein lysine methyltransferases (PKMTs), is emerging as a prominent posttranslation modification that regulates different signaling pathways (*17*–*21*). The monomethyltransferase SET domain–containing protein 6 (SETD6) was originally identified to directly methylate RelA [p65, a subunit of nuclear factor κB (NF-κB) complex] and, thereby, to suppress the activation of NF-κB target genes (*22*). SETD6 was also shown to play an important role in cell cycle regulation, oxidative stress response, WNT signaling, embryonic stem cell self-renewal, nuclear hormone receptor signaling, and cellular proliferation in several cellular models (*23*–*28*). The fact that BRD4 is tightly linked to the regulation of many of these processes raised the intriguing hypothesis of potential cellular and functional cross-talk between SETD6 and BRD4.

Here, we demonstrate that SETD6 binds and methylates the lysine-99 (K99) residue of BRD4 on chromatin. RNA sequencing (RNA-seq) experiments revealed that BRD4 methylation regulates the expression of genes that are involved in translation and inhibits total mRNA translation in cells. Mechanistically, our data suggest that SETD6-mediated methylation of BRD4 at K99 affects neither the integrity of ribosome complexes nor the interaction of BRD4 with acetylated H4 on chromatin. We provide evidence that supports a model where BRD4, independent of its methylation at K99, is present on chromatin on genes that are involved in translation. Our data rather suggest that BRD4 methylation state on chromatin selectively determines the recruitment of the transcription factor E2F1 to these target genes and, hence, their transcriptional activation.

RESULTS

SETD6 methylates and binds BRD4 in vitro and in cells

To test whether BRD4 is methylated by SETD6 in vitro, we performed a radioactive methylation assay in the presence of truncated His-tagged BRD4 (1-477aa) and GST SETD6 (Fig. 1A). The results suggest that SETD6 methylates BRD4. BRD4 contains two bromodomains, BD1 and BD2 (see diagram in Fig. 2A), and we used these recombinant fragments to initially map the methylation site. As shown in Fig. 1B, our results suggest that SETD6 directly and specifically methylates the BD1 domain, but not BD2. To determine whether BRD4 is methylated while associated with chromatin, we overexpressed Flag BRD4 (1-477aa), together with HA-tagged SETD6 in human embryonic kidney (HEK) 293T cells. The cells were then submitted to chromatin extraction followed by immunoprecipitation using protein-protein

[1]The Shraga Segal Department of Microbiology, Immunology and Genetics, Ben-Gurion University of the Negev, P.O.B. 653, Be'er-Sheva 84105, Israel. [2]National Institute for Biotechnology in the Negev, Ben-Gurion University of the Negev, P.O.B. 653, Be'er-Sheva 84105, Israel. [3]GSK Cellzome GmbH, Functional Genomics R&D, 69117 Heidelberg, Germany. [4]Sir Peter MacCallum Department of Oncology and Centre for Cancer Research, University of Melbourne, Melbourne, Australia. [5]Department of Life Sciences, Ben-Gurion University of the Negev, Be'er-Sheva 84105, Israel. [6]Structural Genomics Consortium, Nuffield Department of Clinical Medicine, University of Oxford, Oxford OX3 7DQ, UK. [7]GSK, Medicines Research Centre, Gunnels Wood Road, Stevenage, Hertfordshire SG1 2NY, UK.
*Corresponding author. Email: ledan@post.bgu.ac.il

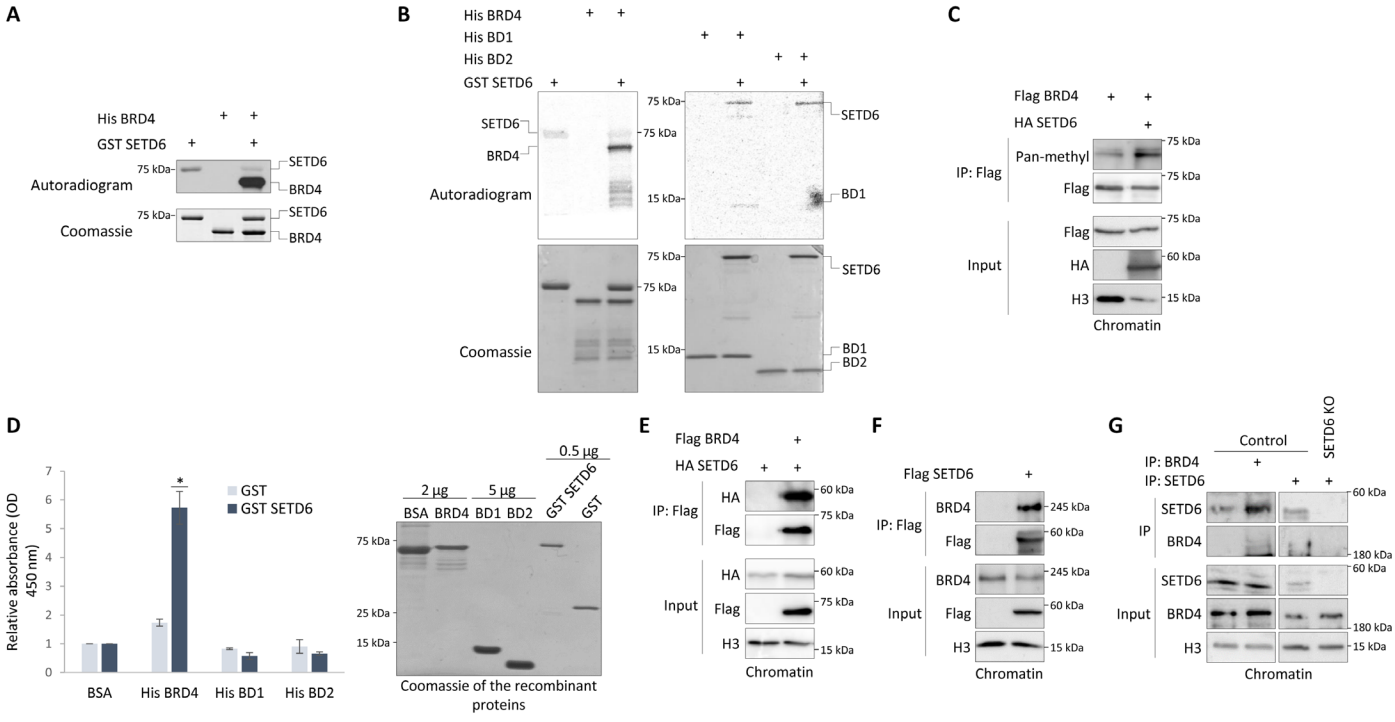

Fig. 1. SETD6 binds and methylates BRD4 in vitro and on chromatin in cells. (**A** and **B**) In vitro methylation of BRD4 by SETD6. Samples were subjected to SDS–polyacrylamide gel electrophoresis (PAGE) followed by exposure to autoradiogram to detect ^{3}H-labeled proteins or Coomassie staining to detect all proteins. (**C**) SETD6 methylates BRD4 in cells. Human embryonic kidney (HEK) 293T wild-type cells were transfected with Flag BRD4 (1-477aa) with or without HA SETD6. Chromatin fractions from HEK293T cells were immunoprecipitated with FLAG-M2 beads, followed by Western blot analysis with indicated antibodies. (**D**) In vitro interaction between SETD6 and BRD4. Enzyme-linked immunosorbent assay (ELISA) was performed with the indicated recombinant proteins. The graph represents relative absorbance normalized to bovine serum albumin (BSA) signal of each condition. Error bars are SD. On the right, Coomassie staining represents all proteins used in this assay. Statistical analysis was performed for three experimental repeats using Student's *t* test. *$P < 0.05$. (**E** to **G**) SETD6 binds BRD4 in cells. Chromatin fractions of HEK293T (E) and MDA-MBA-231 (F and G) cells, transfected or not as indicated, were isolated, immunoprecipitated, and submitted to Western blot analysis with the indicated antibodies.

chromatin immunoprecipitation (ChIP) protocol, as previously described (*29*). Western blotting with a pan-methyl antibody revealed that BRD4 methylation level was increased on chromatin in the presence of SETD6 (Fig. 1C).

We next investigated the physical interaction between BRD4 and SETD6. A direct interaction between the proteins was tested in an enzyme-linked immunosorbent assay (ELISA). In these experiments, recombinant His BRD4 (1-477aa), His BD1, His BD2, or bovine serum albumin (BSA) as negative control was immobilized on a 96-well plate, followed by incubation with recombinant glutathione *S*-transferase (GST) SETD6 or GST (Fig. 1D). The results suggest that SETD6 directly binds BRD4, but not through its bromodomains. Co-IP experiments were then performed and showed an interaction in the chromatin fraction between both overexpressed and tagged proteins in HEK293T cells (Fig. 1E), between overexpressed SETD6 and endogenous BRD4 in MDA-MB-231 cells (Fig. 1F), and also between endogenous SETD6 and BRD4 in MDA-MB-231 cells (Fig. 1G). Collectively, our data suggest that SETD6 methylates and binds BRD4 in vitro and in cells directly on chromatin.

SETD6 methylates BRD4 at lysine-99

These findings prompted us to map BRD4 methylation site by SETD6. Using mass spectrometry analysis, we identified mono-methylation on lysine-99 (K99), which is located inside the BD1 domain (Fig. 2A and fig. S1, A and B). Extracted ion chromatograms of the corresponding tryptic peptides showed an incubation time–dependent increase of the mono-methylation in the presence of the cosubstrate *S*-adenosylmethionine (SAM), confirming that site occupancy is dependent on the enzymatic activity of SETD6 (fig. S1, C and D). To validate these findings, we performed an in vitro methylation reaction using recombinant His-Sumo BRD4 wild type and BRD4 K99R proteins as substrates. The methylation signal of the mutant BRD4 K99R was significantly lower compared to BRD4 wild type, suggesting that K99 is the primary methylation site targeted by SETD6 (Fig. 2B). While the mass spectrometry analysis identified only one methylation site, the remaining signal in the BRD4 K99R mutant may suggest that there are additional methylation sites on BRD4. Catalytically inactive SETD6 mutant (Y285A) (*22*, *30*) served as a negative control for the reaction. These results were confirmed in a semi–in vitro methylation assay where immunoprecipitated overexpressed Flag BRD4 wild type or K99R from the chromatin fraction was subjected to an in vitro methylation assay in the presence of recombinant SETD6 (Fig. 2C). To test BRD4 methylation in cells, we generated site- and state-specific antibodies to recognize methylated BRD4 at K99. We used two rabbit polyclonal antibodies, U292 and U293, which were raised against two BRD4 mono-methylated peptides at K99 (see Materials and Methods). Both antibodies could specifically detect methylated BRD4 peptides (1 and 2) in a dose-dependent

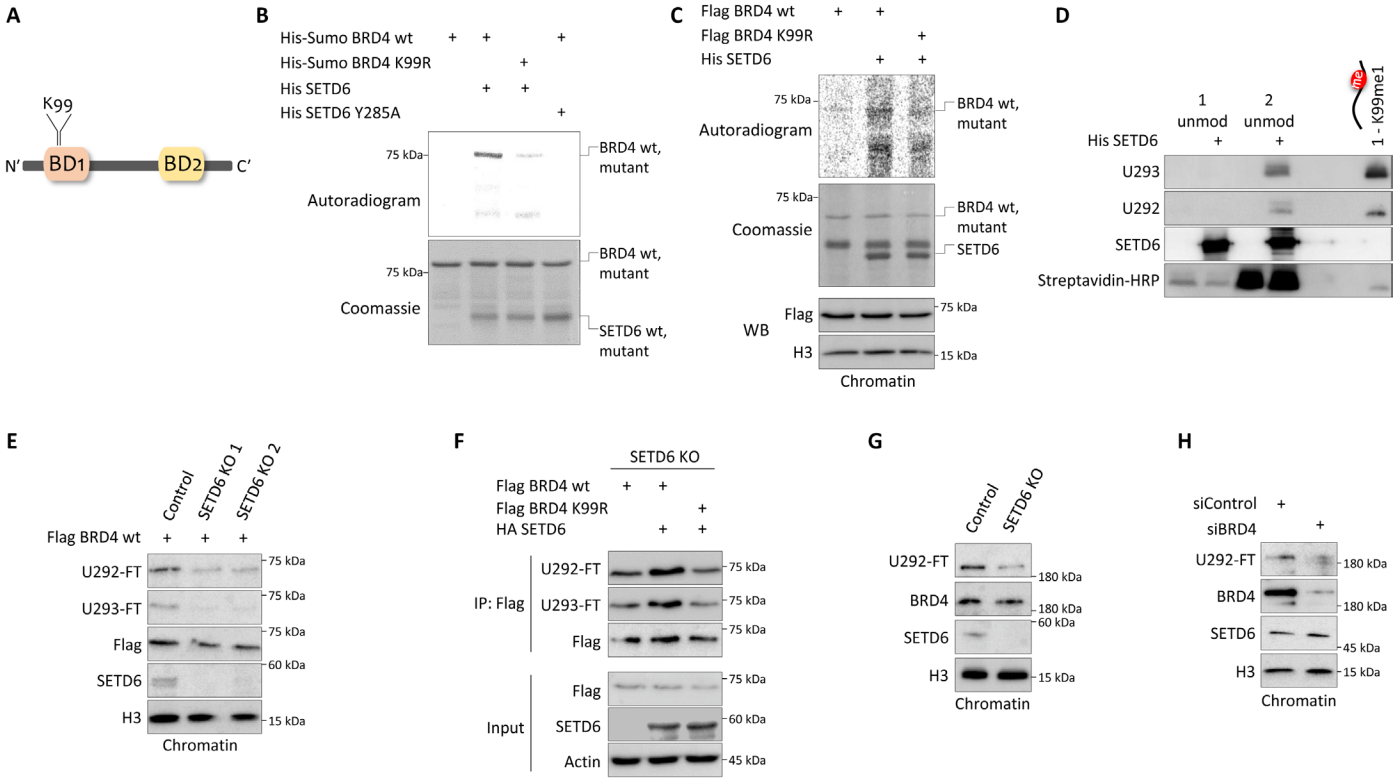

Fig. 2. SETD6 methylates BRD4 at K99. (**A**) Illustration of truncated BRD4 (1-477aa) with identified lysine-99 (K99) as the methylation site by SETD6. (**B**) SETD6 methylates BRD4 at K99 in vitro. In vitro methylation reaction with the indicated recombinant proteins was incubated in the presence of ^{3}H-labeled SAM. Samples were then resolved by SDS-PAGE followed by exposure to autoradiogram detection or Coomassie staining. (**C**) Semi–in vitro methylation assay. Immunoprecipitated Flag-BRD4 from HEK293T SETD6 knockout (KO) cell chromatin fractions were subjected to radioactive in vitro methylation assay. (**D**) In vitro validation of BRD4 K99me1 antibodies (U292 and U293). Unmodified biotin-labeled BRD4 peptides were incubated with or without His SETD6 in the presence of cold *S*-adenosylmethionine (SAM) followed by Western blot (WB) analysis with the indicated antibodies.1-K99me1 peptide served as positive control. (**E** to **H**) Validation of BRD4 K99me1 antibodies (U292-FT and U293-FT) in cells under different experimental conditions. (E) Chromatin fraction of MDA-MB-231 control and CRISPR SETD6 KO cells overexpressing Flag BRD4 wild type (wt). (F) Flag immunoprecipitation of MDA-MB-231 CRISPR SETD6 KO cells overexpressing Flag BRD4 wild type or Flag BRD4 K99R (1-477aa). (G) Chromatin fraction of MDA-MB-231 control and CRISPR SETD6 KO. (H) Chromatin fraction of MDA-MB-231 wild-type cells treated with siRNA control or BRD4 for 48 hours.

manner and not the unmodified or scrambled peptides (fig. S2A). In addition, both antibodies specifically recognized the methylation induced by His SETD6 on peptide 2, but not on peptide 1, suggesting that SETD6 is able to methylate peptide 2, but not peptide 1 (Fig. 2D and Materials and Methods for peptide sequences), most likely due to changes in their conformational recognition following the variation in their amino acid content (see Materials and Methods). K99me1 peptide was used as positive control in this experiment. Furthermore, in an in vitro methylation reaction using recombinant proteins, while cross-reactivity of both antibodies with unmethylated BRD4 was observed, a notable increase in the signal was found when SETD6 was added to the reaction (fig. S2B). In addition, an increase in BRD4 K99 methylation signal was observed using the U293 antibody when Flag BRD4 was immunoprecipitated from MDA-MB-231 cells and incubated with recombinant His SETD6 (fig. S2C). We next used these antibodies to determine whether BRD4 is methylated at K99 in cells. Here, we used U292-FT and U293-FT antibodies, which had been subjected to further affinity purification. Depletion of SETD6 in MDA-MB-231 cells with two independent single-clone guide RNAs (gRNAs) resulted in a decrease in the methylation of Flag BRD4 on chromatin (Fig. 2E). Moreover, in a rescue experiment that was performed in the SETD6 knockout (KO) cells, addition of HA SETD6 increased the methylation of BRD4 wild type but not the K99 mutant (Fig. 2F), suggesting that the methylation of BRD4 at K99 is SETD6 dependent. A substantial reduction in the methylation of endogenous BRD4 was observed in the SETD6 KO cells on chromatin (Fig. 2G). To confirm that the signal in cells is specific to BRD4, endogenous BRD4 was knocked down with small interfering RNA (siRNA), and the level of BRD4 methylation at the chromatin was further assessed with the K99me antibody (U292-FT). As shown in Fig. 2H, silencing of BRD4 correlates with a reduction of its methylation level. Together, these data suggest that SETD6 specifically methylates BRD4 at K99 in vitro and in cells.

SETD6-mediated methylation of BRD4 at K99 regulates the expression of genes involved in mRNA translation

We hypothesized that BRD4 methylation at K99 by SETD6 may serve as a regulatory mechanism to mediate BRD4 function to govern gene expression programs. To address this hypothesis, we designed an RNA-seq experiment using MDA-MB-231 control and SETD6 CRISPR KO or knockdown (KD) cells (Fig. 3A) and MDA-MB-231 cells stably expressing an empty plasmid, Flag BRD4 wild type (1-477aa), or Flag

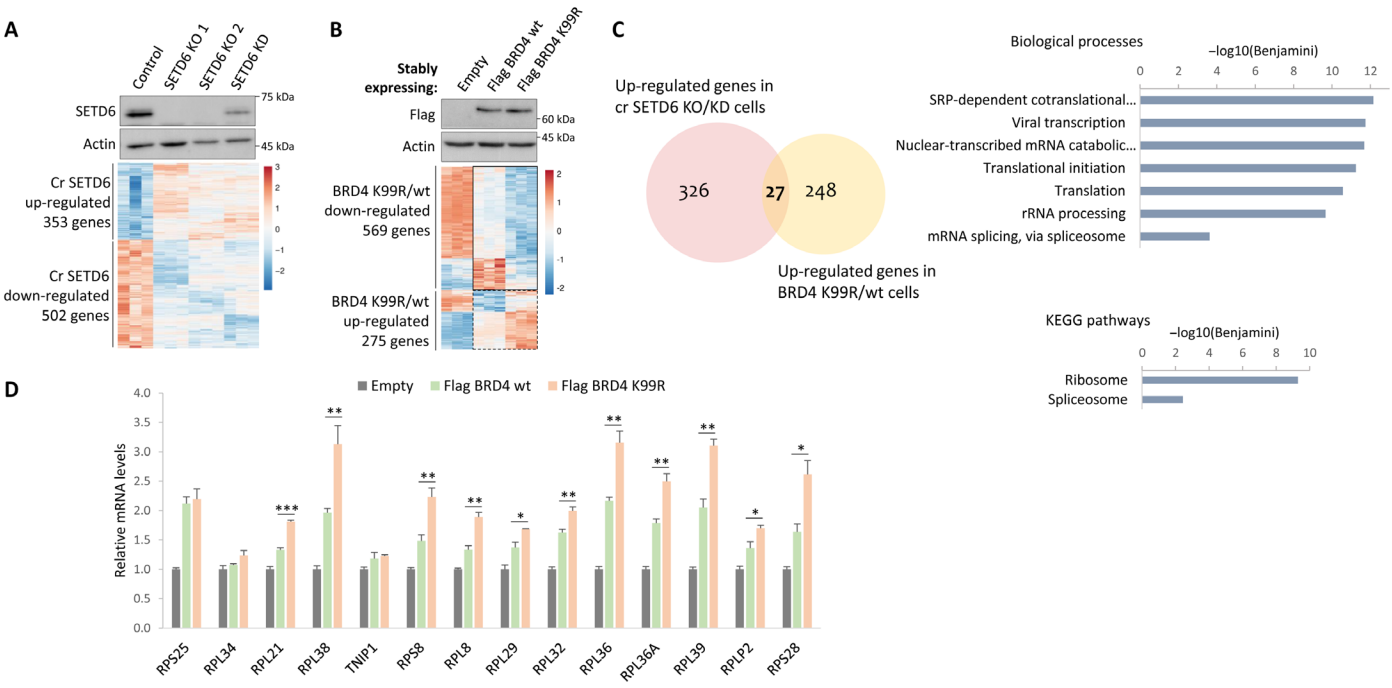

Fig. 3. SETD6-mediated methylation of BRD4 at K99 regulates the expression of genes involved in mRNA translation. (**A** and **B**) MDA-MB-231 (A) CRISPR control and SETD6 KO/KD or (B) stably expressing Flag BRD4 wild-type or Flag BRD4 K99R cells were subjected to Western blot indicating SETD6 (A) or Flag BRD4 protein levels (B) in the cells (top). Bottom: Heatmap of differentially expressed up- and down-regulated genes from RNA-seq in all the indicated cells. Orange and blue colors represent higher and lower expression, respectively. (**C**) Common up-regulated (*27*) CRISPR SETD6 KO/KD–dependent and BRD4 K99R–dependent genes were analyzed using the DAVID database for biological processes and Kyoto Encyclopedia of Genes and Genomes (KEGG) pathways (on the right). Pathways shown are based on the Benjamini-corrected *P* value of <0.05. (**D**) Validation of RNA-seq experiments. mRNA was extracted from MDA-MB-231 cells, and transcript levels were determined by quantitative polymerase chain reaction (qPCR). mRNA levels were normalized to glyceraldehyde-3-phosphate dehydrogenase (GAPDH) and then to empty cells. Error bars are SEM. Statistical analysis was performed for three experimental repeats using one-way ANOVA. **P* < 0.05, ***P* < 0.01, and ****P* < 0.001.

BRD4 K99R mutant (Fig. 3B). Total RNAs were extracted from these cells, and triplicate samples were sent for sequencing. We found 353 up-regulated and 502 down-regulated genes in the CRISPR SETD6 KO/KD cells (Fig. 3A, heatmap). We identified 275 up-regulated and 569 down-regulated genes in the cells stably expressing Flag BRD4 K99R in comparison to Flag BRD4 wild type–expressing cells (Fig. 3B, heatmap). Enrichment testing for biological processes and Kyoto Encyclopedia of Genes and Genomes (KEGG) pathways was then carried out to further explore the link between SETD6 and BRD4 methylation at K99. To do so, we compared the down- and up-regulated genes in the SETD6 KO/KD cells to the cells stably expressing the BRD4 K99R mutant. Both conditions mimic the situation by which BRD4 is not methylated. We found diverse pathways, such as cell-matrix adhesion and focal adhesions in the common 67 down-regulated genes (fig. S3). In the common 27 up-regulated gene analysis, we noticed that mRNA translation and ribosomal RNA (rRNA) processing pathways were significantly up-regulated in cells lacking SETD6 or in the cells stably expressing BRD4 K99R mutant (Fig. 3C). The expression of these specific genes was then validated by quantitative polymerase chain reaction (qPCR). As shown in Fig. 3D, a significant elevation in the expression of these genes was found in cells stably expressing BRD4 K99R, which represents an unmethylated state of BRD4. The fact that also the wild-type BRD4 increases expression of those genes indicates that this might be a dosage effect. Collectively, these experiments suggest that SETD6-mediated methylation of BRD4 at K99 negatively affects the expression of genes involved in mRNA translation.

BRD4 methylation at K99 inhibits translation

We hypothesized that unmethylated BRD4 enhances translation in cells. To test this hypothesis, we measured total protein synthesis using the SUnSET method (*31*). In this approach, puromycin (an analog of aminoacyl transfer RNAs) is incorporated into newly synthesized polypeptide chains, and the resulting proteins are detected by Western blot using anti-puromycin antibody. Protein synthesis was elevated in the SETD6 KO cells (two independent gRNAs) compared to control cells, suggesting that depletion of SETD6 enhances mRNA translation (Fig. 4A). In a rescue experiment in MDA-MB-231 SETD6 KO cells, addition of exogenous HA SETD6 to the cells reduced the total protein synthesis (Fig. 4B), which suggests that this phenomenon is SETD6 dependent. We next measured total protein synthesis in MDA-MB-231 cells stably expressing an empty plasmid, Flag BRD4 wild type, or Flag BRD4 K99R mutant. Consistent with our working hypothesis, we found that the protein synthesis is elevated in BRD4 K99R compared to cells stably expressing BRD4 wild type or empty cells (Fig. 4C). Elevated protein synthesis was also observed in cells overexpressing K99R BRD4 long isoform (Fig. 4D). Having demonstrated that SETD6 regulates protein synthesis in a BRD4-dependent manner, we next asked whether BRD4 interacts with monosomes or polysomes. To this end, we performed

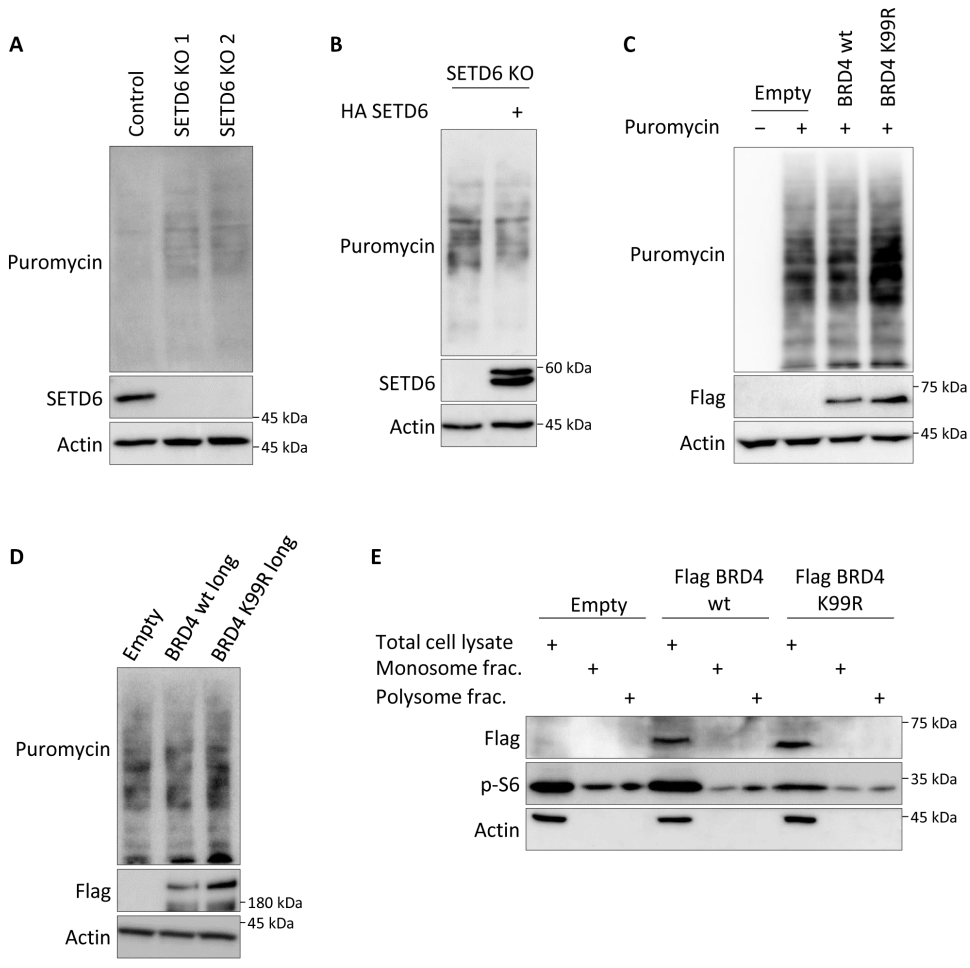

Fig. 4. BRD4 methylation at K99 inhibits translation. (**A** to **D**) Translation assay (SUnSET). (A) MDA-MB-231 control and CRISPR SETD6 KO (two independent gRNAs) cells. (B) MDA-MB-231 CRISPR SETD6 KO cells with or without overexpressed HA SETD6. (C) MDA-MB-231 cells stably expressing empty plasmid, Flag BRD4 wild type, or Flag BRD4 K99R (1-477aa). (D) MDA-MB-231 wild-type cells overexpressing empty plasmid, Flag BRD4 wild type, or Flag BRD4 K99R (long isoform). Cells were incubated with puromycin and then cell extracts were submitted to Western blot to detect protein synthesis using anti-puromycin antibody. (**E**) Polysome profiling. Monosome and polysome fractions were extracted from MDA-MB-231 cells stably expressing empty plasmid, Flag BRD4 wild type, or Flag BRD4 K99R (1-477aa). The fractions and total cell lysates, served as control, were submitted to Western blot analysis with anti-Flag antibody. Actin served as loading control. Phosphorylated S6 (p-S6) served as control for polysome profiling method.

a polysome profiling of cells stably expressing an empty plasmid, Flag BRD4 wild type, or Flag BRD4 K99R. Total cell lysates from these cells and the monosome and polysome fractions were analyzed by Western blot (Fig. 4E). Our results suggest that BRD4 wild type or BRD4 K99R mutant is not part of the monosome or polysome fractions. These results support the observation that the translation regulation by SETD6-mediated methylation of BRD4 at K99 is carried out by controlling the transcription of genes that are then involved in translation.

BRD4 methylation at K99 does not regulate the interaction with acetylated H4 at chromatin

The bromodomains of BRD4 specifically recognize and bind acetylated lysine residues of targeted histone and non-histone proteins (*3*–*7*). Having demonstrated that SETD6 methylates BRD4 at K99, within the BD1 domain, raises the intriguing hypothesis that BRD4 methylation regulates its association with the chromatin and specifically with acetylated histones. To address this hypothesis, we tested whether BRD4 wild type binds acetylated H4 differently than BRD4 K99R in a co-IP experiment using a specific validated antibody that recognizes a tetra-acetylated histone H4 at lysines K5, K8, K12, and K16 (*32*, *33*). To observe a specific signal from this antibody, the addition of the deacetylase inhibitor trichostatin A (TSA) was required to increase global acetylation levels. As expected, without TSA treatment, we could not detect interaction between BRD4 and the tetra-acetylated H4 (Fig. 5A, second lane). Treatment with TSA led to a specific interaction of BRD4 with the tetra-acetylated H4. However, we could not see any difference between wild-type BRD4 and the K99R mutant in their ability to bind tetra-acetylated H4 (Fig. 5A, two lanes on the right), which was not the case for the BRD4 N140F mutant, known for its inability to bind the tetra-acetylated H4 (fig. S4) (*34*). Furthermore, similar binding of tetra-acetylated H4 to endogenous BRD4 was observed in both control and SETD6 KO MDA-MB-231 cells when BRD4 was immunoprecipitated (Fig. 5B).

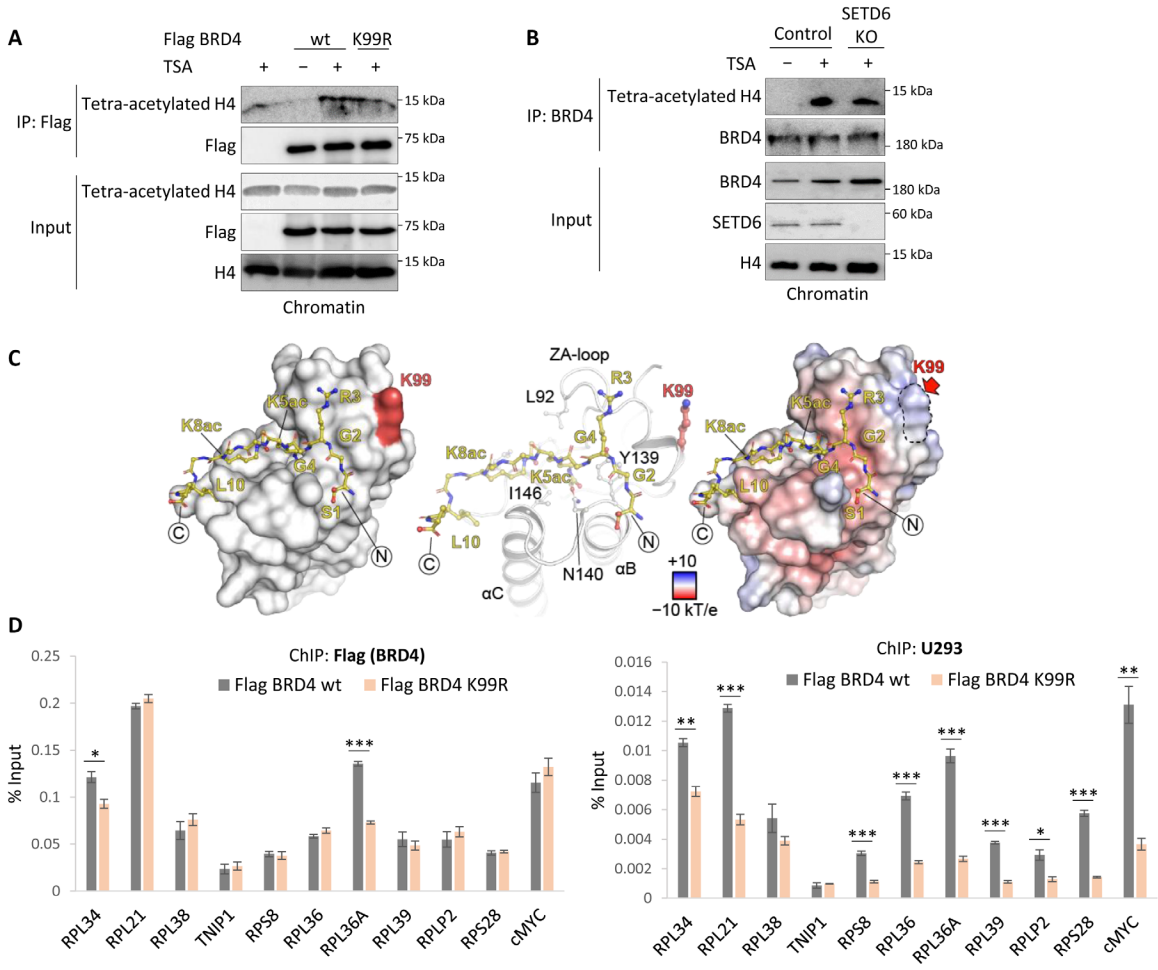

Fig. 5. BRD4 K99me does not affect its binding to acetylated H4. (**A** and **B**) MDA-MB-231 wild-type cells were transfected as indicated and treated with TSA for 4 hours. Chromatin fractions were immunoprecipitated with indicated antibodies, followed by Western blot analysis with anti–tetra-acetylated H4 antibody. (**C**) Left: Topology of the H4K5ac/K8ac (H4 residues 1 to 11) peptide binding to BRD4/BD1. The peptide termini are annotated and the location of K99 is highlighted in red [Protein Data Bank (PDB) ID: 3UVW (*34*)]. Middle: Crystal structure of the complex of BRD4/BD1 with an H4 (1 to 11) K5ac/K8ac peptide (PDB: 3UVW) shown in ribbon and stick representation. Residues that initiate contact are annotated and K99 is shown in red (same orientation as on the left). Right: Binding of H4 (1 to 11) K5ac/K8ac onto the surface of BRD4/BD1. Protein charge distribution is plotted on the surface of BRD4/BD1, highlighting the extensive electrostatic nature of the interaction. Location of K99 is highlighted in red. (**D**) ChIP assay for MDA-MB-231 wild-type cells overexpressing Flag BRD4 wild type or Flag BRD4 K99R (1-477aa) using FLAG-M2 (left) or U293 antibody (right). Graphs show percent input of the quantified DNA. Error bars are SEM. Statistical analysis was performed for three experimental repeats using Student's *t* test. $^{*}P < 0.05$, $^{**}P < 0.01$, and $^{***}P < 0.001$.

To support these observations, analysis of the available structural data in the model of BRD4/BD1 bound to H4K5ac/K8ac showed that there is no direct interaction between any of the histone peptide residues and K99, which is located behind the ZA loop (Fig. 5C). While we cannot rule out that methylation of this site would potentially affect the surface properties of the protein, our cellular data support a model where Kac recognition is not directly affected by K99me. On the molecular level, ChIP experiments (Fig. 5D) for Flag BRD4 wild type and K99R mutant confirmed that both unmethylated and methylated BRD4 (Fig. 5D, right, U293 antibody) are present at chromatin on most of the different genes that are involved in translation that were tested. From this set of experiments, we concluded that the methylation of BRD4 at K99 does not affect the overall recognition and binding to acetylated H4 at chromatin.

BRD4 methylation at K99 controls a selective binding to E2F1 to regulate the transcription of genes that are involved in mRNA translation

Our results so far suggest that SETD6 methylates BRD4 at K99 to regulate the expression of ribosomal target genes and total mRNA translation. We also found that BRD4 methylation does not have a direct role in the assembly of the ribosome complex or in the association with acetylated histone H4 through its bromodomains. We next wanted to understand the underlying mechanism by which SETD6 and the methylation of BRD4 at K99 regulate mRNA translation. To do so, we performed a ChIP-X enrichment analysis (ChEA), which is a gene set enrichment analysis tool to identify a putative binding of transcription factors to a given set of target genes based on published data such as ChIP-chip, ChIP-seq, and ChIP-PET experiments (*35*). We performed the ChEA analysis on the set of

genes that were up-regulated in the BRD4 K99R RNA-seq results shown in Fig. 3B, which displayed an enrichment in processes linked to translation regulation. Of the 275 up-regulated genes, the ChEA analysis identified a significant enrichment (adjusted *P* value of 2.1×0^{-7}) for the transcription factor E2F1 in 100 of them (Fig. 6A). This finding, together with previous reports showing that E2F1 regulates translation (*36*–*38*), implies that methylation of BRD4 at K99 orchestrates a selective binding to E2F1 to regulate transcription of genes involved in mRNA translation. To address this hypothesis, we first performed a translation assay using the SUnSET method and found that in the presence of overexpressed E2F1 in MDA-MB-231 cells, there is an increase in mRNA translation in a dose-dependent manner (fig. S5A). We then performed an ELISA to test for a direct interaction between E2F1 and BRD4 and to determine whether the methylation of BRD4 by SETD6 attenuates this interaction. Our results indicate that BRD4 binds E2F1 and that this interaction is reduced when BRD4 is methylated after the addition of recombinant SETD6 (Fig. 6B). Increased E2F1 binding was observed when BRD4 was incubated with the catalytically inactive SETD6 Y285A, confirming that this phenomenon is methylation dependent in vitro (fig. S5B, and parallel Coomassie stains for the recombinant proteins used in the reaction in fig. S5C). To test whether methylation of BRD4 selectively regulates the interaction with E2F1 in cells, we immunoprecipitated Flag BRD4 in control and SETD6 KO cells. Consistent with our working model, overexpressed E2F1 binds methylated BRD4 in the control cells; however, a stronger interaction was observed in SETD6 KO cells where BRD4 is not methylated (Fig. 6C). Moreover, in a rescue experiment, we found that overexpression of HA SETD6 in the SETD6 KO cells attenuates the interaction between the overexpressed long isoform of BRD4 and endogenous E2F1 (Fig. 6D). These results further support that BRD4 methylation at K99 selectively regulates the binding of E2F1 to specific target genes. In a ChIP experiment, we found a significant enrichment for binding of Flag E2F1 to target genes involved in translation (RNA-seq; Fig. 3, A to C) in cells overexpressing BRD4 K99R compared to wild-type cells (Fig. 6E). E2F1 enrichment correlates well with a significant increase in the transcription of most of the target genes that were tested in cells that express BRD4 K99R mutant, together with HA-E2F1 (Fig. 6F and Western blot in fig. S5D). Together, our data support a new model by which SETD6 methylation of BRD4 at K99 plays a role in the recruitment of E2F1 to mRNA translation–related target genes for the regulation of their transcription (Fig. 6G).

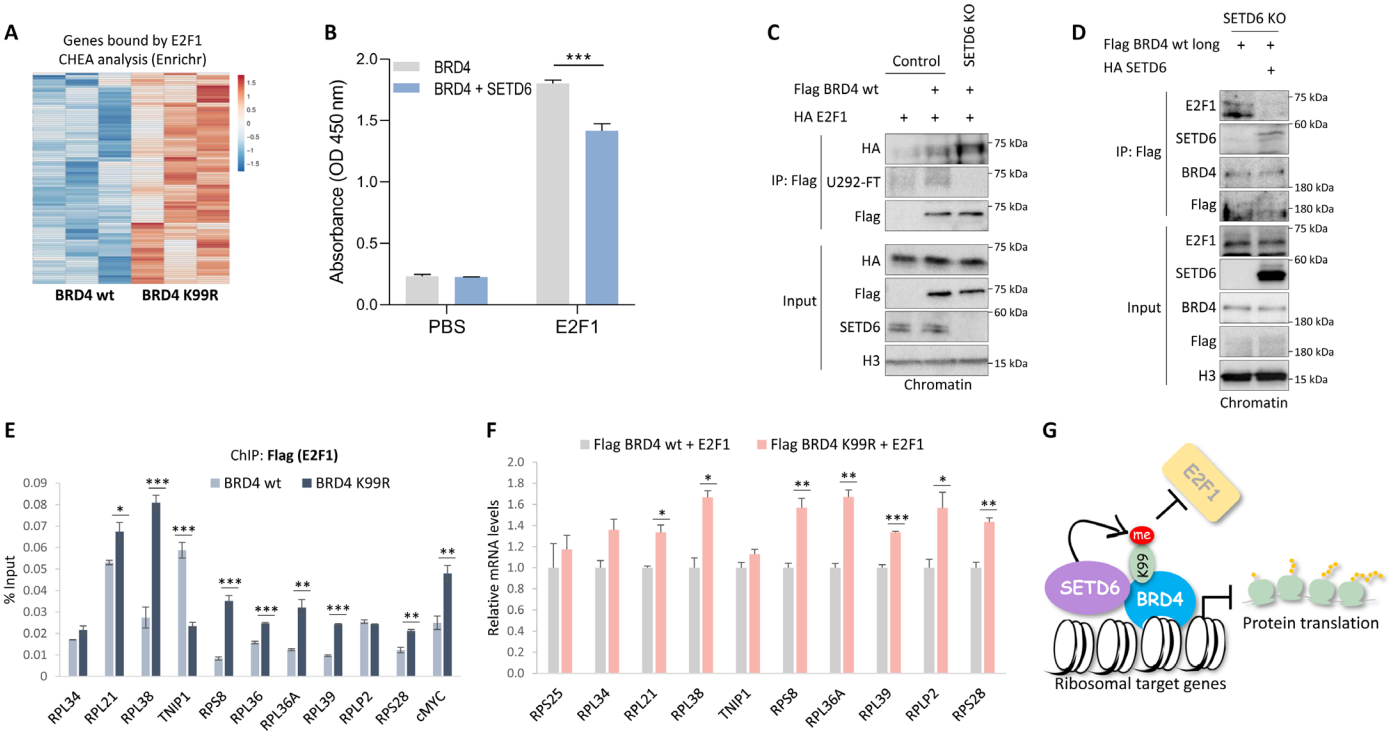

Fig. 6. BRD4 methylation at K99 controls selective binding to E2F1 to regulate transcription of genes involved in mRNA translation. (**A**) Heatmap representing 100 enriched genes for E2F1 transcription factor, analyzed by ChEA. Orange and blue colors represent higher and lower expression, respectively. (**B**) ELISA was performed with the indicated recombinant proteins preincubated in an in vitro methylation assay. Graph represents absorbance compared to phosphate-buffered saline (PBS) signal. Error bars are SD. Statistical analysis was performed for three experimental repeats using Student's *t* test. ***$P < 0.001$. OD, optical density. (**C** and **D**) MDA-MB-231 cells overexpressing the indicated plasmids were subjected to chromatin isolation and immunoprecipitation with FLAG-M2 antibody. (**E**) ChIP assay for MDA-MB-231 overexpressing Flag E2F1, with HA BRD4 wild type or HA BRD4 K99R (1-477aa). Graphs show percent input of the quantified DNA. Error bars are SEM. Statistical analysis was performed for three experimental repeats using Student's *t* test. *$P < 0.05$, **$P < 0.01$, and ***$P < 0.001$. (**F**) mRNA was extracted from MDA-MB-231 cells and transcript levels were determined by qPCR. Error bars are SEM. Statistical analysis was performed for three experimental repeats using Student's *t* test. *$P < 0.05$, **$P < 0.01$, and ***$P < 0.001$. (**G**) Schematic model illustrating the decrease of E2F1 recruitment to the chromatin and down-regulation of translation-related target gene transcription following BRD4 methylation at K99 by SETD6.

DISCUSSION

The epigenetic reader BRD4 is essential for coordinating gene expression by binding to acetylated proteins at chromatin to recruit specific factors to regulate transcription (*2*, *39*–*41*). BRD4 has been used as a therapeutic target for various inhibitors that displace it from the chromatin (*4*, *8*–*16*). However, BRD4 upstream regulation by posttranslational modifications is poorly understood. Here, we identify BRD4 as a novel substrate for methylation by SETD6. Our model suggests that methylated BRD4 at K99 inhibits the selective recruitment of the transcription factor E2F1 to translation-related target genes, leading to global translation repression (Fig. 6G).

A role for BRD4 in translation has been described before. It was shown that BRD4 down-regulation decreases the synthesis of pre-rRNA (*42*). This study found that BRD2 and BRD4 directly bind rDNA (ribosomal DNA) promoters (*42*). BRD2 and BRD4 presence at rDNA promoters is mediated by LYAR (cell growth–regulating nucleolar protein) and UBF (upstream binding factor). Together with the histone acetyltransferase KAT7, BRD2 and BRD4 promote the acetylation of histones H3 and H4 at rDNA sites to enhance rDNA transcription. Our RNA-seq experiments revealed changes in the expression of target genes that are involved in translation and splicing (Fig. 3C). However, we cannot rule out the possibility that these changes result from a compensatory effect caused by reduced activity of BRD4 following its methylation. In future experiments, using the specific K99-methyl antibody developed in our study, it would be interesting to test what the methylation status of BRD4 is in these processes and to determine whether BRD4 methylation represents another layer of regulation to fine-tune the activation/repression of genes involved in mRNA translation via recruitment of different accessory transcription factors.

E2F1, a cell proliferation and cell cycle regulator, has been reported to induce ribosome biogenesis (*36*). While BRD4 methylation does not affect ribosome association, our data suggest that SETD6 functions as a molecular switch that determines the methylation state of BRD4, which will consequently affect E2F1 recruitment to genes that are involved in mRNA translation. While the study presented here is restricted to two cell types, it would be instructive to test whether there is a tight correlation between SETD6 expression level and BRD4 methylation in other cellular systems and whether, at the genomic level, BRD4 K99 methylation correlates with the requirement for E2F1 on its target genes.

In addition to BRD4, the lysine residue K99 is conserved among the other BET family proteins, BRD2 and BRD3, but not the testis-specific BRDT (*43*). This may indicate that, similarly to BRD4, methylation of BRD2 and BRD3, which are ubiquitously expressed in various tissues (*44*, *45*), may regulate their activity. If that is the case, future experiments will allow us to determine whether it has a redundant or a specific effect. Phosphosite database interrogation (*46*) indicates that K99 in BRD4 and the corresponding lysine (K75) in BRD3 may also be subject to ubiquitination. While this observation is based only on proteomic discovery mass spectrometry experiments and was not validated biochemically by conventional methods, it still raises a very intriguing model of a competition between two different modifications.

Enhanced mRNA translation may lead to increased proliferation and transformation. Dysregulation of transcription of genes involved in mRNA translation may lead to genomic instability and cancer (*36*, *47*). Our findings suggest that selective transcription activation is mediated by a methylation signaling initiated by SETD6, which, in turn, regulates the recruitment of E2F1 to chromatin, based on the methylation status of BRD4. This molecular multistep mode of action may therefore represent a new direction for the development of new therapeutic applications.

MATERIALS AND METHODS

Plasmids

Truncated BRD4 1-477aa and BRD4 long isoform were amplified using primers indicated in Table 1. For bacterial expression, BRD4 1-477aa was cloned into pET-Duet and pET-Sumo plasmids. To generate BRD4 K99R mutation, site-directed mutagenesis on the BRD4 1-477aa vector was performed using primers indicated in Table 1. Mutated BRD4 K99R fragment was subcloned into BRD4 long isoform using Kpn I restriction enzyme. Both mutants were sequenced for confirmation. BRD4 K99R 1-477aa mutant was cloned into pET-Sumo plasmid. BRD4 1-477aa wild type and K99R mutant were cloned into pcDNA3.1 3×Flag, pcDNA3.1 3×HA, and pWZL-Flag plasmids. BRD4 long isoform wild type or K99R mutant was also cloned into pcDNA3.1 3×Flag plasmid.

SETD6 sequence was amplified by PCR and subcloned into pcDNA3.1 3×Flag and pcDNA3.1 3×HA plasmids, as previously described (*25*). For recombinant protein purification, SETD6 was cloned into pET-Duet plasmid. pET-Duet SETD6 Y285A plasmid was generated as described previously by Weil *et al.* (*30*). E2F1 sequence was amplified using primers indicated in Table 1. E2F1 was cloned into pET-Duet, pcDNA3.1 3×Flag, and pcDNA3.1 3×HA plasmids.

Cell lines, transfection, infection, and treatment

HEK293T and human breast adenocarcinoma cells (MDA-MB-231) were maintained in Dulbecco's modified Eagle's medium (Sigma-Aldrich, D5671) with 10% fetal bovine serum (Gibco), penicillin-streptomycin (Sigma-Aldrich, P0781), L-glutamine (2 mg/ml; Sigma-Aldrich, G7513), and nonessential amino acids (Sigma-Aldrich, M7145), at 37°C in a humidified incubator with 5% CO_2 as previously described (*49*). Cell transfection was performed using Mirus reagents (*Trans*IT-LT1 or *Trans*IT-X2), according to the manufacturer's instructions. CRISPR-Cas9 SETD6 KO or KD cells were generated as previously described (*25*).

Table 1. Primers for cloning and mutagenesis. FW, forward; Rev, reverse.

Name	Sequence (5′ to 3′)
BRD4 FW	TTAGGCGCGCCTCTGCGGAGAGCGGCCC
BRD4 1-477 Rev	GCCTTAATTAATCAGGTGGGAGGGGGCAC
BRD4 long Rev	GCCTTAATTAATCAGAAAAGATTTTCTTCAAATATTGACAATAG
BRD4 K99R FW	GAACCTCCCTGATTACTATAGGATCATTAAAACGCCTATGGATATG
BRD4 K99R Rev	CCATAGGCGTTTTAATGATCCTATAGTAATCAGGGAGGTTCAGC
E2F1 FW	TTAGGCGCGCCGCCTTGGCCGGGGCCCC
E2F1 Rev	GGCTTAATTAATCAGAAATCCAGGGGGGTGAGG

For stable transfection in MDA-MB-231 cell line, retroviruses were produced by transfecting HEK293T cells with the indicated pWZL constructs (empty, Flag BRD4 1-477aa wild type, or Flag BRD4 K99R) and with plasmids encoding VSV and gag-pol. Target cells were infected with the viral supernatants and selected with hygromycin B (650 μg/ml; TOKU-E). For TSA treatment, cells were treated for 4 hours with 1 μM compound or with dimethyl sulfoxide as control. TSA was provided by D. Toiber (Ben-Gurion University, Israel). For siRNA treatment, MDA-MB-231 cells were transfected with 50 nM ON-TARGETplus siControl or siBRD4 (Dharmacon, D-001810-10-05 and L-004937-00-0005, respectively) for 48 hours.

Recombinant proteins and peptides

Escherichia coli Rosetta transformed with a plasmid expressing His-tagged or His-Sumo–tagged BRD4 1-477aa wild type, BRD4 K99R mutant, E2F1, SETD6 wild type, or SETD6 Y285A mutant was grown in LB medium. Bacteria were harvested by centrifugation after isopropyl-β-D-thiogalactopyranoside induction and lysed by sonication on ice (25% amplitude, 1 min total, 10/5-s ON/OFF). His-tagged proteins were purified using Ni–nitrilotriacetic acid beads (Pierce) or on a HisTrap column (GE Healthcare) with the ÄKTA gel filtration system. Proteins were eluted by 0.5 M imidazole followed by dialysis to 10% glycerol in phosphate-buffered saline (PBS) as previously described (*48*). Recombinant GST SETD6 was expressed and purified as previously described (*22*). Purified domains His BD1, His BD2, and BRD4 were discussed before (*49*). BRD4 biotin-labeled peptide sequences were as follows: 1-unmod, N′-CDAVKLNLPDYY-KIIKTPM-C′; 1-K99me1, N′-CDAVKLNLPDYYK$_{me1}$IIKTPM-C′; 2-unmod, N′-LPDYYKIIKTPMDMGTIKKRLEC-C′; 2-K99me1, N′-LPDYYK$_{me1}$IIKTPMDMGTIKKRLEC-C′.

Antibodies, Western blot analysis, and immunoprecipitation

Primary antibodies used were as follows: anti-Flag (Sigma-Aldrich, F1804), anti-HA (Millipore, 05-904), anti-actin (Abcam, ab3280), anti-GST (Abcam, ab9085), anti-SETD6 (GeneTex, GTX629891), anti-BRD4 (Bethyl Laboratories, A700-004), puromycin (DSHB, PMY-2A4), p-6S (Cell Signaling Technology, 2215), anti-E2F1 (Cell Signaling Technology, 3742), anti–tetra-acetylated H4 (Abcam, ab177790), and anti-histone3 (H3) (Abcam, ab10799). H4 (Abcam, ab10158) was provided by A. Aharoni from Ben-Gurion University, Israel. Horseradish peroxidase (HRP)–conjugated secondary antibodies, goat anti-rabbit, goat anti-mouse, and streptavidin-HRP were obtained from Jackson ImmunoResearch (111-035-144, 115-035-062, and 016-030-084, respectively) as previously described (*48*). Anti–pan-methyl (methylated lysine antibody, HRP) was purchased from ImmuneChem (ICP0502).

For Western blot analysis, cells were homogenized and lysed in radioimmunoprecipitation assay (RIPA) buffer [50 mM tris-HCl (pH 8), 150 mM NaCl, 1% Nonidet P-40, 0.5% sodium deoxycholate, 0.1% SDS, 1 mM dithiothreitol (DTT), and 1:100 protease inhibitor mixture (Sigma-Aldrich)]. Samples were resolved on SDS–polyacrylamide gel electrophoresis (PAGE), followed by Western blot analysis. For immunoprecipitation, proteins extracted from cells were incubated for 2 hours at room temperature with FLAG-M2 magnetic beads (Sigma-Aldrich, M8823) or overnight at 4°C with FLAG-M2 beads (Sigma-Aldrich, A2220) or preconjugated A/G agarose beads (Santa Cruz Biotechnology, SC-2003) with antibody of interest. The beads were then washed three times with RIPA buffer and submitted to SDS-PAGE and Western blot analysis.

Polyclonal antibody generation

The following peptides were used to immunize two rabbits, where both animals received both peptides: CDAVKLNLPDYYK$_{me1}$IIKTPM (peptide 1) and LPDYYK$_{me1}$IIKTPMDMGTIKKRLEC (peptide 2) (Abcam, EMEA). All animal studies were ethically reviewed and carried out in accordance with Animals (Scientific Procedures) Act 1986 and the GSK Policy on the Care, Welfare, and Treatment of Animals. Antibody U292 resulted from affinity purification on peptide 1, and U293 was purified on peptide 2. On the basis of initial results, the U292 and U293 antibodies were further optimized to improve their selectivity for methylated over unmethylated BRD4 at K99 by further affinity purification of the flow-through fractions. The flow-through from U292 was purified on peptide 2 and the flow-through from U293 was purified on peptide 1. The refined antibodies are referred to as U292-FT and U293-FT.

In vitro methylation assay

Methylation assay reactions contained 4 μg of His or His-Sumo BRD4 1-477aa wild type, BRD4 K99R mutant, 1 μg of His BD1 or BD2, and 4 μg of His SETD6 or GST SETD6, 2 mCi of ^{3}H-labeled SAM (Perkin-Elmer, AdoMet), and PKMT buffer [20 mM tris-HCl (pH 8), 10% glycerol, 20 mM KCl, and 5 mM $MgCl_2$]. The reaction tubes were incubated overnight at 30°C. The reactions were resolved by SDS-PAGE for Coomassie staining (Expedeon, InstantBlue) or autoradiography. For the nonradioactive (cold) methylation assay, the ^{3}H-labeled SAM was switched to 300 μM cold SAM (Abcam, ab142221).

Semi–in vitro methylation assay

Cells were transfected with Flag BRD4 wild type or K99R plasmids. Chromatin fractions [extracted according to the protein-protein ChIP (ppChIP) protocol, see below] or cell lysates were immunoprecipitated with FLAG-M2 beads overnight at 4°C. The samples were then washed three times with RIPA buffer and once with PKMT buffer, followed by an in vitro radioactive or cold methylation assay overnight at 30°C, with or without 4 μg of His SETD6. The reactions were resolved by SDS-PAGE for Western blot analysis, Coomassie staining, or autoradiography.

Mass spectrometry

Samples of nonradioactive methylation assay containing 3 μg of His BRD4 and 4 μg of GST SETD6 were incubated with 3.2 mM SAM for different periods of time (0.5, 1, 2, 6, and 24 hours) at 30°C. An additional sample without SAM served as reference. The experiment was performed in duplicate. Samples were then digested with trypsin and submitted for liquid chromatography–tandem mass spectrometry analysis. Mass spectrometry analysis was performed with a Thermo Fisher Scientific Q-Exactive mass spectrometer (Thermo Fisher Scientific) coupled online to a nano-flow high-performance liquid chromatography system. Only in the 24-hour samples was an increased ratio of methylated/nonmethylated peptide (LNLPDYYK) identified. Mascot 2.5 (Matrix Science, Boston, MA) was used for protein identification; in a first search, 30 parts per million peptide precursor mass and 30 mDa HCD (higher-energy collisional dissociation) mass tolerance for fragment ions were used for recalibration followed by a database search using a 10 parts per million mass tolerance for peptide precursors and 20 mDa (HCD) mass tolerance for fragment ions. The search database consisted of a customized version of the SwissProt sequence database combined with a decoy version of this database created using scripts

supplied by Matrix Science, and lysine mono-methylation was used as a variable modification. Extracted ion chromatograms were generated with the Xcalibur software.

Enzyme-linked immunosorbent assay

His BRD4 (2 μg), His BD1 (5 μg), His BD2 (5 μg), or BSA diluted in PBS were added to a 96-well plate (Greiner Microlon) and incubated for 1 hour at room temperature, followed by blocking with 3% BSA for 30 min. Then, the plate was covered with 0.5 μg of GST SETD6 or GST protein (negative control) for 1 hour at room temperature. Plates were then washed and incubated with primary antibody (anti-GST, 1:4000 dilution), followed by incubation with HRP-conjugated secondary antibody (goat anti-rabbit, 1:2000 dilution) for 1 hour. Last, trimethylboron reagent and then 1 N H_2SO_4 were added; the absorbance at 450 nm was detected using a Tecan Infinite M200 plate reader. In BRD4-E2F1, ELISA conditions were as follows: His-Sumo BRD4 and His SETD6 wild type or Y285A mutant were incubated with 60 μM cold SAM at 30°C for 5 hours. The plate was covered with the reactions for 1 hour at room temperature, followed by blocking with 3% BSA overnight at 4°C. Then, the plate was covered with 1 μg of His E2F1 or 1% BSA in PBS for 2 hours. The plate was probed with anti-E2F1 primary antibody (1:1000). Signal detection was done as described above.

RNA extraction and real-time qPCR

Total RNA was extracted using the NucleoSpin RNA Kit (Macherey-Nagel). Two hundred nanograms of the extracted RNA was reverse-transcribed to complementary DNA (cDNA) using the iScript cDNA Synthesis Kit (Bio-Rad) according to the manufacturer's instructions. Real-time qPCR was performed using the UPL probe library system (Roche) in a LightCycler 480 System (Roche) as previously described (*48*). The real-time qPCR primers were designed using the universal probe library assay design center (Roche) and University of California, Santa Cruz Genome Bioinformatics (Table 2). All samples were amplified in triplicate in a 384-well plate using the following cycling conditions: 10 min at 95°C, 45 cycles of 10 s at 95°C, 30 s at 60°C, and 1 s at 72°C, followed by 30 s at 40°C. Glyceraldehyde-3-phosphate dehydrogenase (GAPDH) expression and the experiment controls were used for gene expression normalization.

Table 2. Primers for qPCR.

Name	Sequence (5′ to 3′)
GAPDH FW	AGCCACATCGCTCAGACAC
GAPDH Rev	GCCCAATACGACCAAATCC
RPS25 FW	TTGTCCGACATCTTGACGAG
RPS25 Rev	TGTCTTTCTTGGCCGACTTT
RPL34 FW	TGAGTAATAAAAATGAAAAGACGCTGT
RPL34 Rev	TGGCTCTCTCAAGCTGAGGT
RPL21 FW	GGTACCTGGGTTCAACTAAAGC
RPL21 Rev	CATAGGGAATAGGTTCCAGCA
RPL38 FW	GACGAAAGGATGCCAAATCT
RPL38 Rev	GTCAGTGATGACCAGGGTGTAA
TNIP1 FW	CAAAGATGAGGAGAAGGCAAG
TNIP1 Rev	CCACATGGTAACGCTCTCCT
RPS8 FW	AGGTTGGACGTGGGGAAT
RPS8 Rev	TCGATGATCCTTGTTTTACGAG
RPL36A FW	TGTGAGTAGACACATTTCAGGCTAA
RPL36A Rev	CACTTAACTCTTAGCAAAGACATCTCA
RPL36 FW	GGAGGAGCTGAGCAACGTA
RPL36 Rev	GGGAGGGGCTCAGTCTTT
RPS28 FW	GGTCTTGGATGTCGGGTTC
RPS28 Rev	AGGAGCATCTCAGTTACGTGTG
RPLP2 FW	ACCGGCTCAACAAGGTTATC
RPLP2 Rev	GCAGCAGAGACGGCTACAG
RPL29 FW	AGGCTCCCAAACGTACCC
RPL29 Rev	CCCATGCAGATGGTAGCC
RPL32 FW	GAAGTTCCTGGTCCACAACG
RPL32 Rev	GAGCGATCTCGGCACAGTA
RPL39 FW	CAGCTTCCCTCCTCTTCCTT
RPL39 Rev	TGGGACGATTTTGCTTTTGT
RPL8 FW	AGAAGACCCGTGTGAAGCTG
RPL8 Rev	CAAGATGGGTTTGTCAATTCG

Chromatin extraction

Chromatin fraction was isolated using ppChIP protocol, modified from a published protocol (*29*). Briefly, cells were cross-linked using 1% formaldehyde (Sigma-Aldrich) added directly to the medium and incubated on a shaking platform for 10 min at room temperature. The cross-linked reaction was stopped by adding 0.125 M glycine for 5 min. Cells were harvested and washed twice with PBS and then lysed in 1 ml of cell lysis buffer [20 mM tris-HCl (pH 8), 85 mM KCl, 0.5% Nonidet P-40, and 1:100 protease inhibitor cocktail] for 10 min on ice. Nuclear pellets were resuspended in 200 μl of nuclei lysis buffer [50 mM tris-HCl (pH 8), 10 mM EDTA, 1% SDS, and 1:100 protease inhibitor cocktail] for 10 min on ice and then sonicated (Bioruptor, Diagenode) at high-power settings for three cycles, 6 min each (30-s ON/OFF). Samples were centrifuged (13,000 rpm, 15 min, 4°C) and the soluble chromatin fraction was collected. For biochemical extraction of the chromatin, cells were harvested and resuspended in buffer A [10 mM Hepes (pH 7.9), 10 mM KCl, 1.5 mM $MgCl_2$, 0.34 M sucrose, and 10% glycerol] supplemented with 0.1% Triton X-100, 1 mM DTT, 1:200 protease inhibitor (PI) mixture, and 100 nM phenylmethylsulfonyl fluoride (PMSF; Sigma-Aldrich). Cells were incubated for 8 min on ice and then centrifuged for 5 min at 1850*g* at 4°C. The pellet was washed once with buffer A supplemented with DTT, PI, and PMSF, and then lysed with buffer B (3 mM EDTA and 0.2 mM EGTA) supplemented with DTT and PI for 30 min on ice. Samples were centrifuged for 5 min at 1850*g* at 4°C to pellet the chromatin fraction. Last, chromatin fraction was solubilized in buffer A with 1:200 benzonase nuclease enzyme (Sigma-Aldrich) and incubated for 15 min at a 37°C shaker. For immunoprecipitation, the soluble chromatin was incubated for 2 hours at room temperature with FLAG-M2 magnetic beads or overnight at 4°C with FLAG-M2 beads or precleared and incubated with Magna ChIP Protein A + G magnetic beads (Millipore, 16-663) with antibody of interest. Samples were washed according to the ppChIP protocol and analyzed by Western blot.

Chromatin preparation and ChIP-qPCR

For chromatin preparation by sonication, cells were prepared as described in the ppChIP protocol, except for the sonication settings, which were set to six cycles, 6 min each cycle (30-s ON/OFF). Chromatin immunoprecipitation was performed as previously described (*50*, *51*). The chromatin fraction was diluted 5× in dilution buffer [20 mM tris-HCl (pH 8), 2 mM EDTA, 150 mM NaCl, 1.84% Triton X-100, and 0.2% SDS]. Chromatin was precleared overnight at 4°C with nProtein A Sepharose 4 Fast Flow Beads (GE Healthcare, 17-5280-01). The precleared sample was then immunoprecipitated in dilution buffer with FLAG-M2 beads or nProtein A Sepharose beads preconjugated with polyclonal rabbit BRD4 K99me1 antibody. The immunoprecipitated complexes were washed once with TSE150 buffer [20 mM tris-HCl (pH 8), 2 mM EDTA, 1% Triton X-100, 0.1% SDS, and 150 mM NaCl], TSE500 buffer [20 mM tris-HCl (pH 8), 2 mM EDTA, 1% Triton X-100, 0.1% SDS, and 500 mM NaCl], buffer 3 [250 mM LiCl, 10 mM tris-HCl (pH 8), 1 mM EDTA, 1% sodium deoxycholate, and 1% Nonidet P-40], and twice with TE buffer [10 mM tris-HCl (pH 8) and 1 mM EDTA]. DNA was eluted with elution buffer (50 mM $NaHCO_3$, 140 mM NaCl, and 1% SDS) containing ribonuclease A (0.2 μg/μl) and proteinase K (0.2 μg/μl). Last, the DNA eluates were decross-linked at 65°C overnight with shaking at 900 rpm and purified by NucleoSpin Gel and PCR Clean-up kit (Macherey-Nagel), according to the manufacturer's instructions. Purified DNA was subjected to qPCR using specific primers (Table 3). Primers were designed on the basis of BRD4 occupancy found in different ChIP-seq data previously published in National Center for Biotechnology Information Gene Expression Omnibus (GEO) datasets by Xiong *et al.* (*52*) (GEO accession: GSE123097), Rhie *et al.* (*53*) (GEO accession: GSE49651), Messier *et al.* (*54*) (GEO accession: GSE69377), and Zanconato *et al.* (*55*) (GEO accession: GSE102406) and viewed using Integrated Genomics Viewer software (*56*). qPCR was preformed using SYBR Green I Master (Roche) in a LightCycler 480 System (Roche). All samples were amplified in triplicate in a 384-well plate using the following cycling conditions: 5 min at 95°C, 45 cycles of amplification; 10 s at 95°C, 10 s at 60°C, and 10 s at 72°C, followed by melting curve acquisition; and 5 s at 95°C, 1 min at 65°C and monitoring up to 97°C, and lastly cooling for 30 s at 40°C. The results were normalized to input DNA and presented as % input.

Table 3. Primers for ChIP-qPCR.

Name	Sequence (5′ to 3′)
cMYC ChIP FW	AATTCCAGCGAGAGGCAGAG
cMYC ChIP Rev	GAAGCCCCCTATTCGCTCC
TNIP1 ChIP FW	GAGGCTCTGGACGATCTGGG
TNIP1 ChIP Rev	CTCCCCGTCCTCGGGTAAG
RPL34 ChIP FW	GTCCTTTGAGCTGGTGTAGGG
RPL34 ChIP Rev	GCTGTGGCTACTCACGGCT
RPL21 ChIP FW	GGCCTCAGAGGTCGTTCATT
RPL21 ChIP Rev	ACATGGTTTAACCCGCCCAT
RPL38 ChIP FW	CGATATTTCGGGGGAGAGCG
RPL38 ChIP Rev	GACCTGCGGGAAACAGTCC
RPS8 ChIP FW	AGCCTACTGAGGAGTCCAGA
RPS8 ChIP Rev	CGAAACCCGAGGGCCAC
RPL36A ChIP FW	GGCCGAGTAACATCCAGCTT
RPL36A ChIP Rev	GTTGATCCCGGCAAGATTGG
RPL36 ChIP FW	AGGTTGGAGGATGGTTGGTT
RPL36 ChIP Rev	GAGAAGGGGCGGAGGTGA
RPS28 ChIP FW	GGAGGGATTAGAGGAGCCAA
RPS28 ChIP Rev	CGTGCACTGTCCCTGAGAA
RPLP2 ChIP FW	CCTTTGGACTCGCTTCGTC
RPLP2 ChIP Rev	GTTCCGGAAGTGACTGCTCT

RNA-seq and data processing

Total RNA was extracted from MDA-MB-231 cells with different treatments, using the NucleoSpin RNA Kit (Macherey-Nagel), according to the manufacturer's instructions. Samples were prepared in triplicate. Barcoded stranded mRNA-seq libraries were prepared at European Molecular Biology Laboratory Genomic Core Facilities (Heidelberg, Germany) from high-quality total RNA samples (~500 ng per sample) using the Illumina TruSeq RNA Sample Preparation v2 Kit in the workflow implemented on the liquid-handling robot Beckman FXP2. Obtained libraries that passed the QC (quality control) step were combined in equimolar amounts into pools of eight libraries; 10 pM solution of each pool was loaded per lane of the Illumina sequencer HiSeq 2500 flow cell and sequenced unidirectionally with the Illumina v4 chemistry, generating ~220 million reads per lane, each 50 bases long, and then aligned to the human genome reference hg38 and quantified.

Bioinformatic analysis

Bioinformatic analysis of the RNA-seq data was carried out using NeatSeq-Flow (*57*) and R. Raw sequence reads underwent quality assessment with FASTQC and MultiQC, followed by quality trimming with Trim Galore!. Clean reads were aligned to the human genome version GRCh38 (Ensembl) using STAR, and gene expression was estimated with RSEM (RNA-Seq by Expectation-Maximization). Subsequent analysis was done for each experiment (CRISPR SETD6 and stable BRD4 cells) separately. For quality assessment, counts underwent variance-stabilizing transformation [DESeq2 (*58*)] and submitted to sample-wise correlation analysis and principal components analysis. Statistical testing for differential expression was carried out using DESeq2, a method specifically tailored for count data by use of negative binomial generalized linear models.

For hierarchical clustering, genes were selected according to the following criteria: in the SETD6 experiment, annotated genes (i.e., having a gene symbol) that were either up-regulated or down-regulated [false discovery rate (FDR)–adjusted P value < 0.05] in all KO/KD treatments versus the control; in the BRD4 experiment, annotated genes in the up-regulated or down-regulated category (FDR-adjusted P value < 0.05) in BRD4 K99R versus BRD4 wild type comparison, and significantly changed (either up- or down-regulated) in BRD4 wild-type versus empty comparison. Hierarchical clustering, after z-scoring of their variance-stabilized expression values, was carried out using the ClustVis web tool (https://biit.cs.ut.ee/clustvis/) (*59*). Enrichment for gene ontology biological processes and KEGG pathways was performed using DAVID (https://david.ncifcrf.gov/) (*60*, *61*).

ChEA was performed using Enrichr database (*62*, *63*). The 275 up-regulated genes identified in RNA-seq of BRD4 K99R compared to BRD4 wild-type cells were submitted to ChEA gene analysis. The

identified genes were visualized in a heatmap, created using the ClustVis web tool (https://biit.cs.ut.ee/clustvis/) (*59*).

Translation assay

For the translation assay performed using the SUnSET method (*31*), cells were treated with puromycin (10 μg/ml) for 10 min. Cells were then lysed in RIPA buffer and submitted to Western blot to detect protein synthesis using anti-puromycin antibody.

Polysome profiling

Polysome profiling was performed as previously published by Liang *et al.* (*64*). Briefly, cells were treated with cycloheximide (100 μg/ml) for 10 min, then washed with PBS that contained cycloheximide (100 μg/ml), and collected by centrifugation at 300*g* for 5 min at 4°C. Cells were lysed in a hypotonic lysis buffer (50 mM tris-base, 2.5 mM $MgCl_2$, 1.5 mM KCl, 5.5% Triton X-100, 0.5% sodium deoxycholate, and 2 mM DTT) containing cycloheximide (100 μg/ml) and RNaseOUT (0.24 U/μl; Thermo Fisher Scientific, 10777019), vortexed, and centrifuged at 17,800*g* for 2 min at 4°C. Fifty microliters of the samples was saved (total cell lysate), and the rest were loaded on the top of a three-layer sucrose gradient tube followed by ultracentrifugation at 36,000 rpm for 2.5 hours at 4°C. Monosome and polysome fractions were collected using a piston gradient collector (Biocomp) fitted with an ultraviolet detector (Tirax). Samples were then dialyzed in PBS buffer and concentrated using Amicon Ultra 0.5-ml Centrifugal Filters (Merck). All samples were resolved on SDS-PAGE and subjected to Western blot analysis.

Statistical analyses

Statistical analyses for all assays were performed with GraphPad Prism software, using Student's two-tailed *t* test (unpaired) and one-way or two-way analysis of variance (ANOVA) with a Tukey's post hoc test.

SUPPLEMENTARY MATERIALS

Supplementary material for this article is available at http://advances.sciencemag.org/cgi/content/full/7/22/eabf5374/DC1

View/request a protocol for this paper from *Bio-protocol*.

REFERENCES AND NOTES

1. J. L. Morgado-Pascual, S. Rayego-Mateos, L. Tejedor, B. Suarez-Alvarez, M. Ruiz-Ortega, Bromodomain and extraterminal proteins as novel epigenetic targets for renal diseases. *Front. Pharmacol.* **10**, 1315 (2019).
2. P. Filippakopoulos, S. Knapp, Targeting bromodomains: Epigenetic readers of lysine acetylation. *Nat. Rev. Drug Discov.* **13**, 337–356 (2014).
3. A. Hajmirza, A. Emadali, A. Gauthier, O. Casasnovas, R. Gressin, M. B. Callanan, BET family protein BRD4: An emerging actor in NFκB signaling in inflammation and cancer. *Biomedicine* **6**, 16 (2018).
4. J. Shi, Y. Wang, L. Zeng, Y. Wu, J. Deng, Q. Zhang, Y. Lin, J. Li, T. Kang, M. Tao, E. Rusinova, G. Zhang, C. Wang, H. Zhu, J. Yao, Y.-X. Zeng, B. M. Evers, M.-M. Zhou, B. P. Zhou, Disrupting the interaction of BRD4 with diacetylated Twist suppresses tumorigenesis in basal-like breast cancer. *Cancer Cell* **25**, 210–225 (2014).
5. Z. Yang, N. He, Q. Zhou, Brd4 recruits P-TEFb to chromosomes at late mitosis to promote G_1 gene expression and cell cycle progression. *Mol. Cell. Biol.* **28**, 967–976 (2008).
6. Z. Yang, J. H. N. Yik, R. Chen, N. He, M. K. Jang, K. Ozato, Q. Zhou, Recruitment of P-TEFb for stimulation of transcriptional elongation by the bromodomain protein Brd4. *Mol. Cell* **19**, 535–545 (2005).
7. M. K. Jang, K. Mochizuki, M. Zhou, H.-S. Jeong, J. N. Brady, K. Ozato, The bromodomain protein Brd4 is a positive regulatory component of P-TEFb and stimulates RNA polymerase II-dependent transcription. *Mol. Cell* **19**, 523–534 (2005).
8. M. A. Dawson, E. J. Gudgin, S. J. Horton, G. Giotopoulos, E. Meduri, S. Robson, E. Cannizzaro, H. Osaki, M. Wiese, S. Putwain, C. Y. Fong, C. Grove, J. Craig, A. Dittmann, D. Lugo, P. Jeffrey, G. Drewes, K. Lee, L. Bullinger, R. K. Prinjha, T. Kouzarides, G. S. Vassiliou, B. J. P. Huntly, Recurrent mutations, including NPM1c, activate a BRD4-dependent core transcriptional program in acute myeloid leukemia. *Leukemia* **28**, 311–320 (2014).
9. O. Gilan, I. Rioja, K. Knezevic, M. J. Bell, M. M. Yeung, N. R. Harker, E. Y. N. Lam, C.-w. Chung, P. Bamborough, M. Petretich, M. Urh, S. J. Atkinson, A. K. Bassil, E. J. Roberts, D. Vassiliadis, M. L. Burr, A. G. S. Preston, C. Wellaway, T. Werner, J. R. Gray, A.-M. Michon, T. Gobbetti, V. Kumar, P. E. Soden, A. Haynes, J. Vappiani, D. F. Tough, S. Taylor, S.-J. Dawson, M. Bantscheff, M. Lindon, G. Drewes, E. H. Demont, D. L. Daniels, P. Grandi, R. K. Prinjha, M. A. Dawson, Selective targeting of BD1 and BD2 of the BET proteins in cancer and immunoinflammation. *Science* **368**, 387–394 (2020).
10. Z. Yao, S. Yang, H. Zhao, H. Yang, X. Jiang, BET inhibitor I-BET151 sensitizes GBM cells to temozolomide via PUMA induction. *Cancer Gene Ther.* **27**, 226–234 (2020).
11. A. Liu, D. Fan, Y. Wang, The BET bromodomain inhibitor i-BET151 impairs ovarian cancer metastasis and improves antitumor immunity. *Cell Tissue Res.* **374**, 577–585 (2018).
12. C. Y. Fong, O. Gilan, E. Y. N. Lam, A. F. Rubin, S. Ftouni, D. Tyler, K. Stanley, D. Sinha, P. Yeh, J. Morison, G. Giotopoulos, D. Lugo, P. Jeffrey, S. C.-W. Lee, C. Carpenter, R. Gregory, R. G. Ramsay, S. W. Lane, O. Abdel-Wahab, T. Kouzarides, R. W. Johnstone, S.-J. Dawson, B. J. P. Huntly, R. K. Prinjha, A. T. Papenfuss, M. A. Dawson, BET inhibitor resistance emerges from leukaemia stem cells. *Nature* **525**, 538–542 (2015).
13. A. Chaidos, V. Caputo, K. Gouvedenou, B. Liu, I. Marigo, M. S. Chaudhry, A. Rotolo, D. F. Tough, N. N. Smithers, A. K. Bassil, T. D. Chapman, N. R. Harker, O. Barbash, P. Tummino, N. Al-Mahdi, A. C. Haynes, L. Cutler, B. C. Le, A. Rahemtulla, I. Roberts, M. Kleijnen, J. J. Witherington, N. J. Parr, R. K. Prinjha, A. Karadimitris, Potent antimyeloma activity of the novel bromodomain inhibitors I-BET151 and I-BET762. *Blood* **123**, 697–705 (2014).
14. M. A. Dawson, R. K. Prinjha, A. Dittmann, G. Giotopoulos, M. Bantscheff, W.-I. Chan, S. C. Robson, C.-w. Chung, C. Hopf, M. M. Savitski, C. Huthmacher, E. Gudgin, D. Lugo, S. Beinke, T. D. Chapman, E. J. Roberts, P. E. Soden, K. R. Auger, O. Mirguet, K. Doehner, R. Delwel, A. K. Burnett, P. Jeffrey, G. Drewes, K. Lee, B. J. P. Huntly, T. Kouzarides, Inhibition of BET recruitment to chromatin as an effective treatment for MLL-fusion leukaemia. *Nature* **478**, 529–533 (2011).
15. J. E. Delmore, G. C. Issa, M. E. Lemieux, P. B. Rahl, J. Shi, H. M. Jacobs, E. Kastritis, T. Gilpatrick, R. M. Paranal, J. Qi, M. Chesi, A. C. Schinzel, M. R. McKeown, T. P. Heffernan, C. R. Vakoc, P. L. Bergsagel, I. M. Ghobrial, P. G. Richardson, R. A. Young, W. C. Hahn, K. C. Anderson, A. L. Kung, J. E. Bradner, C. S. Mitsiades, BET bromodomain inhibition as a therapeutic strategy to target c-Myc. *Cell* **146**, 904–917 (2011).
16. P. Filippakopoulos, J. Qi, S. Picaud, Y. Shen, W. B. Smith, O. Fedorov, E. M. Morse, T. Keates, T. T. Hickman, I. Felletar, M. Philpott, S. Munro, M. R. McKeown, Y. Wang, A. L. Christie, N. West, M. J. Cameron, B. Schwartz, T. D. Heightman, N. L. Thangue, C. A. French, O. Wiest, A. L. Kung, S. Knapp, J. E. Bradner, Selective inhibition of BET bromodomains. *Nature* **468**, 1067–1073 (2010).
17. H. Alam, B. Gu, M. G. Lee, Histone methylation modifiers in cellular signaling pathways. *Cell. Mol. Life Sci.* **72**, 4577–4592 (2015).
18. R. Hamamoto, V. Saloura, Y. Nakamura, Critical roles of non-histone protein lysine methylation in human tumorigenesis. *Nat. Rev. Cancer* **15**, 110–124 (2015).
19. E. M. Cornett, L. Ferry, P.-A. Defossez, S. B. Rothbart, Lysine methylation regulators moonlighting outside the epigenome. *Mol. Cell* **75**, 1092–1101 (2019).
20. D. Levy, Lysine methylation signaling of non-histone proteins in the nucleus. *Cell. Mol. Life Sci.* **76**, 2873–2883 (2019).
21. D. Han, M. Huang, T. Wang, Z. Li, Y. Chen, C. Liu, Z. Lei, X. Chu, Lysine methylation of transcription factors in cancer. *Cell Death Dis.* **10**, 290 (2019).
22. D. Levy, A. J. Kuo, Y. Chang, U. Schaefer, C. Kitson, P. Cheung, A. Espejo, B. M. Zee, C. L. Liu, S. Tangsombatvisit, R. I. Tennen, A. Y. Kuo, S. Tanjing, R. Cheung, K. F. Chua, P. J. Utz, X. Shi, R. K. Prinjha, K. Lee, B. A. Garcia, M. T. Bedford, A. Tarakhovsky, X. Cheng, O. Gozani, Lysine methylation of the NF-κB subunit RelA by SETD6 couples activity of the histone methyltransferase GLP at chromatin to tonic repression of NF-κB signaling. *Nat. Immunol.* **12**, 29–36 (2011).
23. M. Feldman, Z. Vershinin, I. Goliand, N. Elia, D. Levy, The methyltransferase SETD6 regulates mitotic progression through PLK1 methylation. *Proc. Natl. Acad. Sci. U.S.A.* **116**, 1235–1240 (2019).
24. R. Yao, Y. Wang, D. Han, Y. Ma, M. Ma, Y. Zhao, J. Tan, J. Lu, G. Xu, X. Li, Lysines 207 and 325 methylation of WDR5 catalyzed by SETD6 promotes breast cancer cell proliferation and migration. *Oncol. Rep.* **40**, 3069–3077 (2018).
25. Z. Vershinin, M. Feldman, A. Chen, D. Levy, PAK4 methylation by SETD6 promotes the activation of the Wnt/β-Catenin pathway. *J. Biol. Chem.* **291**, 6786–6795 (2016).
26. A. Chen, M. Feldman, Z. Vershinin, D. Levy, SETD6 is a negative regulator of oxidative stress response. *Biochim. Biophys. Acta* **1859**, 420–427 (2016).
27. D. J. O'Neill, S. C. Williamson, D. Alkharaif, I. C. Monteiro, M. Goudreault, L. Gaughan, C. N. Robson, A. C. Gingras, O. Binda, SETD6 controls the expression of estrogen-responsive genes and proliferation of breast carcinoma cells. *Epigenetics* **9**, 942–950 (2014).
28. O. Binda, A. Sevilla, G. LeRoy, I. R. Lemischka, B. A. Garcia, S. Richard, SETD6 monomethylates H2AZ on lysine 7 and is required for the maintenance of embryonic stem cell self-renewal. *Epigenetics* **8**, 177–183 (2013).

29. R. M. Ricke, A.-K. Bielinsky, Easy detection of chromatin binding proteins by the histone association assay. *Biol. Proced. Online* **7**, 60–69 (2005).
30. L. E. Weil, Y. Shmidov, M. Kublanovsky, D. Morgenstern, M. Feldman, R. Bitton, D. Levy, Oligomerization and auto-methylation of the human lysine methyltransferase SETD6. *J. Mol. Biol.* **430**, 4359–4368 (2018).
31. E. K. Schmidt, G. Clavarino, M. Ceppi, P. Pierre, SUnSET, a nonradioactive method to monitor protein synthesis. *Nat. Methods* **6**, 275–277 (2009).
32. L. Handoko, B. Kaczkowski, C. C. Hon, M. Lizio, M. Wakamori, T. Matsuda, T. Ito, P. Jeyamohan, Y. Sato, K. Sakamoto, S. Yokoyama, H. Kimura, A. Minoda, T. Umehara, JQ1 affects BRD2-dependent and independent transcription regulation without disrupting H4-hyperacetylated chromatin states. *Epigenetics* **13**, 410–431 (2018).
33. J.-P. Lambert, S. Picaud, T. Fujisawa, H. Hou, P. Savitsky, L. Uusküla-Reimand, G. D. Gupta, H. Abdouni, Z.-Y. Lin, M. Tucholska, J. D. R. Knight, B. Gonzalez-Badillo, N. St-Denis, J. A. Newman, M. Stucki, L. Pelletier, N. Bandeira, M. D. Wilson, P. Filippakopoulos, A.-C. Gingras, Interactome rewiring following pharmacological targeting of BET bromodomains. *Mol. Cell* **73**, 621–638.e17 (2019).
34. P. Filippakopoulos, S. Picaud, M. Mangos, T. Keates, J.-P. Lambert, D. Barsyte-Lovejoy, I. Felletar, R. Volkmer, S. Müller, T. Pawson, A.-C. Gingras, C. H. Arrowsmith, S. Knapp, Histone recognition and large-scale structural analysis of the human bromodomain family. *Cell* **149**, 214–231 (2012).
35. A. Lachmann, H. Xu, J. Krishnan, S. I. Berger, A. R. Mazloom, A. Ma'ayan, ChEA: Transcription factor regulation inferred from integrating genome-wide ChIP-X experiments. *Bioinformatics* **26**, 2438–2444 (2010).
36. S. Vadivel Gnanasundram, R. Fåhraeus, Translation stress regulates ribosome synthesis and cell proliferation. *Int. J. Mol. Sci.* **19**, 3757 (2018).
37. S. Real, N. Meo-Evoli, L. Espada, A. Tauler, E2F1 regulates cellular growth by mTORC1 signaling. *PLOS ONE* **6**, e16163 (2011).
38. O. Ayrault, L. Andrique, P. Séité, Involvement of the transcriptional factor E2F1 in the regulation of the rRNA promoter. *Exp. Cell Res.* **312**, 1185–1193 (2006).
39. A. Zippo, R. Serafini, M. Rocchigiani, S. Pennacchini, A. Krepelova, S. Oliviero, Histone crosstalk between H3S10ph and H4K16ac generates a histone code that mediates transcription elongation. *Cell* **138**, 1122–1136 (2009).
40. E. P. Blankenhorn, Comparative immunogenetics of the major histocompatibility complex. *Immunol. Ser.* **43**, 287–318 (1989).
41. H. J. Trappe, C. A. Hartwig, H. Klein, P. Wenzlaff, P. R. Lichtlen, Incidence of sudden cardiac death in patients with 2-vessel coronary disease in relation to anatomy and rhythm profile. *Z. Kardiol.* **77**, 1–8 (1988).
42. K. Izumikawa, H. Ishikawa, H. Yoshikawa, S. Fujiyama, A. Watanabe, H. Aburatani, H. Tachikawa, T. Hayano, Y. Miura, T. Isobe, R. J. Simpson, L. Li, J. Min, N. Takahashi, LYAR potentiates rRNA synthesis by recruiting BRD2/4 and the MYST-type acetyltransferase KAT7 to rDNA. *Nucleic Acids Res.* **47**, 10357–10372 (2019).
43. S.-Y. Wu, C.-M. Chiang, The double bromodomain-containing chromatin adaptor Brd4 and transcriptional regulation. *J. Biol. Chem.* **282**, 13141–13145 (2007).
44. A. Stathis, F. Bertoni, BET proteins as targets for anticancer treatment. *Cancer Discov.* **8**, 24–36 (2018).
45. E. Shang, G. Salazar, T. E. Crowley, X. Wang, R. A. Lopez, X. Wang, D. J. Wolgemuth, Identification of unique, differentiation stage-specific patterns of expression of the bromodomain-containing genes *Brd2, Brd3, Brd4*, and *Brdt* in the mouse testis. *Gene Expr. Patterns* **4**, 513–519 (2004).
46. P. V. Hornbeck, B. Zhang, B. Murray, J. M. Kornhauser, V. Latham, E. Skrzypek, PhosphoSitePlus, 2014: Mutations, PTMs and recalibrations. *Nucleic Acids Res.* **43**, D512–D520 (2015).
47. D. Ruggero, P. P. Pandolfi, Does the ribosome translate cancer? *Nat. Rev. Cancer* **3**, 179–192 (2003).
48. Z. Vershinin, M. Feldman, D. Levy, PAK4 methylation by the methyltransferase SETD6 attenuates cell adhesion. *Sci. Rep.* **10**, 17068 (2020).
49. C.-w. Chung, H. Coste, J. H. White, O. Mirguet, J. Wilde, R. L. Gosmini, C. Delves, S. M. Magny, R. Woodward, S. A. Hughes, E. V. Boursier, H. Flynn, A. M. Bouillot, P. Bamborough, J.-M. G. Brusq, F. J. Gellibert, E. J. Jones, A. M. Riou, P. Homes, S. L. Martin, I. J. Uings, J. Toum, C. A. Clément, A.-B. Boullay, R. L. Grimley, F. M. Blandel, R. K. Prinjha, K. Lee, J. Kirilovsky, E. Nicodeme, Discovery and characterization of small molecule inhibitors of the BET family bromodomains. *J. Med. Chem.* **54**, 3827–3838 (2011).
50. S. Mishra, C. Van Rechem, S. Pal, T. L. Clarke, D. Chakraborty, S. D. Mahan, J. C. Black, S. E. Murphy, M. S. Lawrence, D. L. Daniels, J. R. Whetstine, Cross-talk between lysine-modifying enzymes controls site-specific DNA amplifications. *Cell* **174**, 803–817.e16 (2018).
51. E. Ainbinder, M. Revach, O. Wolstein, S. Moshonov, N. Diamant, R. Dikstein, Mechanism of rapid transcriptional induction of tumor necrosis factor alpha-responsive genes by NF-κB. *Mol. Cell. Biol.* **22**, 6354–6362 (2002).
52. L. Xiong, F. Wu, Q. Wu, L. Xu, O. K. Cheung, W. Kang, M. T. Mok, L. L. M. Szeto, C.-Y. Lun, R. W. Lung, J. Zhang, K. H. Yu, S.-D. Lee, G. Huang, C.-M. Wang, J. Liu, Z. Yu, D.-Y. Yu, J.-L. Chou, W.-H. Huang, B. Feng, Y.-S. Cheung, P. B. Lai, P. Tan, N. Wong, M. W. Chan, T. H. Huang, K. Y. Yip, A. S. Cheng, K.-F. To, Aberrant enhancer hypomethylation contributes to hepatic carcinogenesis through global transcriptional reprogramming. *Nat. Commun.* **10**, 335 (2019).
53. S. K. Rhie, D. J. Hazelett, S. G. Coetzee, C. Yan, H. Noushmehr, G. A. Coetzee, Nucleosome positioning and histone modifications define relationships between regulatory elements and nearby gene expression in breast epithelial cells. *BMC Genomics* **15**, 331 (2014).
54. T. L. Messier, J. A. Gordon, J. R. Boyd, C. E. Tye, G. Browne, J. L. Stein, J. B. Lian, G. S. Stein, Histone H3 lysine 4 acetylation and methylation dynamics define breast cancer subtypes. *Oncotarget* **7**, 5094–5109 (2016).
55. F. Zanconato, G. Battilana, M. Forcato, L. Filippi, L. Azzolin, A. Manfrin, E. Quaranta, D. D. Biagio, G. Sigismondo, V. Guzzardo, P. Lejeune, B. Haendler, J. Krijgsveld, M. Fassan, S. Bicciato, M. Cordenonsi, S. Piccolo, Transcriptional addiction in cancer cells is mediated by YAP/TAZ through BRD4. *Nat. Med.* **24**, 1599–1610 (2018).
56. J. T. Robinson, H. Thorvaldsdottir, W. Winckler, M. Guttman, E. S. Lander, G. Getz, J. P. Mesirov, Integrative genomics viewer. *Nat. Biotechnol.* **29**, 24–26 (2011).
57. M. Sklarz, L. Levin, M. Gordon, V. Chalifa-Caspi, NeatSeq-Flow: A lightweight high-throughput sequencing workflow platform for non-programmers and programmers alike. *bioRxiv* , 173005 (2018).
58. M. I. Love, W. Huber, S. Anders, Moderated estimation of fold change and dispersion for RNA-seq data with DESeq2. *Genome Biol.* **15**, 550 (2014).
59. T. Metsalu, J. Vilo, ClustVis: A web tool for visualizing clustering of multivariate data using principal component analysis and heatmap. *Nucleic Acids Res.* **43**, W566–W570 (2015).
60. D. W. Huang, B. T. Sherman, R. A. Lempicki, Systematic and integrative analysis of large gene lists using DAVID bioinformatics resources. *Nat. Protoc.* **4**, 44–57 (2009).
61. D. W. Huang, B. T. Sherman, R. A. Lempicki, Bioinformatics enrichment tools: Paths toward the comprehensive functional analysis of large gene lists. *Nucleic Acids Res.* **37**, 1–13 (2009).
62. M. V. Kuleshov, M. R. Jones, A. D. Rouillard, N. F. Fernandez, Q. Duan, Z. Wang, S. Koplev, S. L. Jenkins, K. M. Jagodnik, A. Lachmann, M. G. McDermott, C. D. Monteiro, G. W. Gundersen, A. Ma'ayan, Enrichr: A comprehensive gene set enrichment analysis web server 2016 update. *Nucleic Acids Res.* **44**, W90–W97 (2016).
63. E. Y. Chen, C. M. Tan, Y. Kou, Q. Duan, Z. Wang, G. V. Meirelles, N. R. Clark, A. Ma'ayan, Enrichr: Interactive and collaborative HTML5 gene list enrichment analysis tool. *BMC Bioinformatics* **14**, 128 (2013).
64. S. Liang, H. M. Bellato, J. Lorent, F. C. S. Lupinacci, C. Oertlin, V. van Hoef, V. P. Andrade, M. Roffe, L. Masvidal, G. N. M. Hajj, O. Larsson, Polysome-profiling in small tissue samples. *Nucleic Acids Res.* **46**, e3 (2018).

Acknowledgments: This paper is dedicated to the memory of my dearest father and an inspiring scientist, Professor Yossi Levy, who passed away while this paper was being peer-reviewed. We thank the Levy lab for technical assistance and helpful discussions. We thank V. Benes and GeneCore for the RNA-seq library preparation and sequencing. **Funding:** This work was supported by grants to D.L. from the Israel Science Foundation (285/14 and 262/18), the Research Career Development Award from the Israel Cancer Research Fund, and the Israel Cancer Association. B.R. acknowledges support from the Israel Science Foundation (1436/19).
Author contributions: Z.V., M.F., and D.L. conceived and designed the majority of the experiments. T.W. and M.B. performed the mass spectrometry analysis, and T.C. and L.E.W. assisted in the experiments to validate the BRD4 K99me1 antibody. K.A. and B.R. performed the polysome profiling experiments, and L.E.W., M.K., and E.A.-S. performed some of the IP experiments. V.C.-C., M.S., E.Y.N.L., and M.A.D. performed the bioinformatic analysis. S.P., P.F., H.D.L., P.G., and M.K. helped with experimental design and provided valuable conceptual input for the study. Z.V., M.F., and D.L. wrote the paper. All authors read and approved the final manuscript. **Competing interests:** The following authors are employees and/or shareholders of GlaxoSmithKline (GSK): T.W., R.A.M., M.B., T.C., H.D.L., P.G., and R.K.P. M.A.D. has been a member of advisory boards for GlaxoSmithKline, CTX CRC, Storm Therapeutics, Celgene, and Cambridge Epigenetix. The other authors declare that they have no competing interests. **Data and materials availability:** All data needed to evaluate the conclusions in the paper are present in the paper and/or the Supplementary Materials. Additional data related to this paper may be requested from the authors.

Submitted 2 November 2020
Accepted 6 April 2021
Published 26 May 2021
10.1126/sciadv.abf5374

Citation: Z. Vershinin, M. Feldman, T. Werner, L. E. Weil, M. Kublanovsky, E. Abaev-Schneiderman, M. Sklarz, E. Y. N. Lam, K. Alasad, S. Picaud, B. Rotblat, R. A. McAdam, V. Chalifa-Caspi, M. Bantscheff, T. Chapman, H. D. Lewis, P. Filippakopoulos, M. A. Dawson, P. Grandi, R. K. Prinjha, D. Levy, BRD4 methylation by the methyltransferase SETD6 regulates selective transcription to control mRNA translation. *Sci. Adv.* **7**, eabf5374 (2021).

BRD4 methylation by the methyltransferase SETD6 regulates selective transcription to control mRNA translation

Zlata Vershinin, Michal Feldman, Thilo Werner, Lital Estrella Weil, Margarita Kublanovsky, Elina Abaev-Schneiderman, Menachem Sklarz, Enid Y. N. Lam, Khawla Alasad, Sarah Picaud, Barak Rotblat, Ruth A. McAdam, Vered Chalifa-Caspi, Marcus Bantscheff, Trevor Chapman, Huw D. Lewis, Panagis Filippakopoulos, Mark A. Dawson, Paola Grandi, Rab K. Prinjha and Dan Levy

Sci Adv **7** (22), eabf5374.
DOI: 10.1126/sciadv.abf5374